Title

A petunia ethylene-responsive element binding factor, PhERF2, plays an important role in antiviral RNA silencing.

Journal

Journal of experimental botany, 67(11)

ISSN

0022-0957

Authors

Sun, Daoyang
Nandety, Raja Sekhar
Zhang, Yanlong
et al.

Publication Date

2016-05-01

DOI

10.1093/jxb/erw155

Peer reviewed

Journal of Experimental Botany, Vol. 67, No. 11 pp. 3353–3365, 2016
doi:10.1093/jxb/erw155 Advance Access publication 19 April 2016
This paper is available online free of all access charges (see http://jxb.oxfordjournals.org/open_access.html for further details)

RESEARCH PAPER

A petunia ethylene-responsive element binding factor, *PhERF2*, plays an important role in antiviral RNA silencing

Daoyang Sun[1,2], Raja Sekhar Nandety[3], Yanlong Zhang[1], Michael S. Reid[2], Lixin Niu[1,*] and Cai-Zhong Jiang[4,*]

[1] Department of Landscape Architecture and Arts, Northwest A&F University, Yangling, Shaanxi 712100, China
[2] Department of Plant Sciences, University of California Davis, Davis, CA 95616, USA
[3] Department of Plant Pathology, University of California Davis, Davis, CA 95616, USA
[4] Crops Pathology and Genetic Research Unit, United States Department of Agriculture, Agricultural Research Service, Davis, CA 95616, USA

* Correspondence: niulixin@nwsuaf.edu.cn or cjiang@ucdavis.edu

Received 24 February 2016; Accepted 24 March 2016

Editor: Lars Hennig, Swedish University of Agricultural Sciences

Abstract

Virus-induced RNA silencing is involved in plant antiviral defense and requires key enzyme components, including RNA-dependent RNA polymerases (RDRs), Dicer-like RNase III enzymes (DCLs), and Argonaute proteins (AGOs). However, the transcriptional regulation of these critical components is largely unknown. In petunia (*Petunia hybrida*), an ethylene-responsive element binding factor, *PhERF2*, is induced by *Tobacco rattle virus* (TRV) infection. Inclusion of a *PhERF2* fragment in a TRV silencing construct containing reporter fragments of *phytoene desaturase* (*PDS*) or *chalcone synthase* (*CHS*) substantially impaired silencing efficiency of both the *PDS* and *CHS* reporters. Silencing was also impaired in *PhERF2*- RNAi lines, where TRV-*PhPDS* infection did not show the expected silencing phenotype (photobleaching). In contrast, photobleaching in response to infiltration with the TRV-*PhPDS* construct was enhanced in plants overexpressing *PhERF2*. Transcript abundance of the RNA silencing-related genes *RDR2*, *RDR6*, *DCL2*, and *AGO2* was lower in *PhERF2*-silenced plants but higher in *PhERF2*-overexpressing plants. Moreover, *PhERF2*-silenced lines showed higher susceptibility to *Cucumber mosaic virus* (CMV) than wild-type (WT) plants, while plants overexpressing *PhERF2* exhibited increased resistance. Interestingly, growth and development of *PhERF2*-RNAi lines were substantially slower, whereas the overexpressing lines were more vigorous than the controls. Taken together, our results indicate that PhERF2 functions as a positive regulator in antiviral RNA silencing.

Key words: Argonaute, *cucumber mosaic virus*, dicer-like enzyme, RNA-dependent RNA polymerase, *tobacco rattle virus*, transcription factor, virus-induced gene silencing.

Introduction

Virus-induced gene silencing (VIGS) is a rapid and effective method for functional characterization of genes in a plant. A recombinant plant virus carrying a host-derived sequence fragment initiates RNA-mediated post-transcriptional gene silencing (PTGS), leading to a transient and specific degradation of the corresponding endogenous mRNA (Kumagai *et al.*, 1995; Dinesh-Kumar *et al.*, 2003; Di Stilio *et al.*, 2010; Tian *et al.*, 2014). A modified *Tobacco rattle virus* (TRV) vector has proved to be an excellent tool for VIGS, due to its wide host range and its ability to infect meristematic cells (Di Stilio *et al.*, 2010). This system is composed of binary transformation plasmids, TRV1 and TRV2, with a region harboring

multiple cloning sites in TRV2 (Liu *et al.*, 2002). The TRV vector has been used successfully for gene function analysis in a number of eudicots, including the commonly used model plants *Arabidopsis* (Turnage *et al.*, 2002; Burch-Smith *et al.*, 2006; Wang *et al.*, 2006), *Nicotiana benthamiana* (Jones *et al.*, 2006; Peterson *et al.*, 2013), *N. tabacum* (Lukhovitskaya *et al.*, 2013), tomato (*Solanum lycopersicum*; Liu *et al.*, 2002; Fu *et al.*, 2005; Jiang *et al.*, 2008; Senthil-Kumar and Mysore, 2011; Fragkostefanakis *et al.*, 2014) and petunia (*Petunia hybrida*; Chen *et al.*, 2004; Spitzer *et al.*, 2007; Broderick and Jones, 2014; Chang *et al.*, 2014). In petunia, silencing of *phytoene desaturase* (*PDS*) or *chalcone synthase* (*CHS*) provides useful phenotypical markers in VIGS studies for functional characterization of genes in leaf and floral tissues, respectively (Chen *et al.*, 2004; Reid *et al.*, 2009; Jiang *et al.*, 2011).

The silencing efficiency of the VIGS system is variable, largely depending on post-inoculation growth temperature and compatibility between the host and the virus. Growth temperature seems to have profound effects on the efficiency of VIGS-based gene silencing. Gene silencing efficiency with a TRV system in tomato is enhanced by low temperature and low humidity (Fu *et al.*, 2006). Low temperature also enhances gene silencing efficiency throughout the life of cotton plants when geminivirus-mediated VIGS is employed (Tuttle *et al.*, 2008). But in contrast, Szittya *et al.* (2003) reported that low temperature inhibits silencing by preventing siRNA generation in *N. benthamiana* protoplasts transfected with *Cymbidium* ringspot virus (CymRSV). The underlying mechanisms of these apparently conflicting findings are not yet well understood. Previously, we tested the effects of silencing *CHS* on a range of purple-flowered petunia cultivars and found significant variations in the silencing phenotypes (Chen *et al.*, 2004; Reid *et al.*, 2009). In studies with silencing *PDS* in tomato we have also observed cultivar-dependent variations in the silencing phenotype (Jiang *et al.*, 2011). Compatibility has limited the range of taxa where TRV-VIGS has successfully been employed. The genetic basis for the variation and limitation is largely unknown.

The antiviral RNA silencing process involves a set of crucial cellular enzymes including RNA-dependent RNA polymerases (RDRs), Dicer-like RNase III enzymes (DCLs), and Argonaute proteins (AGOs). These components contribute to the generation, cleavage of template double-stranded RNA (dsRNA), and interaction with virus-derived small interfering RNA (vsiRNA), respectively. The vsiRNA is incorporated into a RNA-induced silencing complex (RISC) for post-transcriptional suppression of the homologous RNA molecules (Burch-Smith *et al.*, 2006; Gould and Kramer, 2007; Jaubert *et al.*, 2011; Tian *et al.*, 2014). In *Arabidopsis thaliana*, four DCLs, six RDRs, and ten AGOs serve as critical components of the silencing machinery (Donaire *et al.*, 2008; Zhang *et al.*, 2012). DCL1 has a unique function for the production of 21-nucleotide (nt) microRNAs (miRNAs) that is required for coordination of the complex biological functions within the plant (Dunoyer *et al.*, 2005). DCL2, DCL3, and DCL4 catalyse exogenous RNAs with double-stranded features into 22-, 24- and 21-nt siRNAs (Dunoyer *et al.*, 2005; Donaire *et al.*, 2008; Axtell, 2013), respectively. Double deficiency of DCL2 and DCL4 confers more susceptibility to RNA virus infection, such as TRV (Deleris *et al.*, 2006). Among the six RDRs, RDR1, RDR2, and RDR6 participate in the defensive response against distinct positive-strand RNA viruses through the biogenesis of viral secondary siRNAs in Arabidopsis (Donaire *et al.*, 2008; Garcia-Ruiz *et al.*, 2010; Wang *et al.*, 2010, 2011). Current evidence indicates that AGO1 is mainly implicated in the miRNAs silencing pathway (Baumberger and Baulcombe, 2005). Loss-of-function mutation in AGO2 results in an impaired resistance to 2b suppressor-deficient *Cucumber mosaic virus* (CMV) (Wang *et al.*, 2011) and *Potato virus X* (PVX) (Jaubert *et al.*, 2011) in Arabidopsis, and *Tomato bushy stunt virus* (TBSV) (Scholthof *et al.*, 2011) in *N. benthamiana*. Both AGO1 and AGO2 proteins bind to vsiRNAs (Zhang *et al.*, 2006; Takeda *et al.*, 2008; Wang *et al.*, 2011), thereby guiding the downstream silencing process in the virus-infected cells. To date, however, few transcription factors have been reported to be involved in the transcriptional regulation of these critical components.

We have used petunia as a model system for our studies of flower senescence. Transcriptome analysis has identified a cluster of genes that are strongly up-regulated during development and senescence of the flowers, including many transcription factors (Wang *et al.*, 2013). We have successfully employed the TRV-based VIGS vector and a visual reporter such as *CHS* to study the function of some of these genes (Chen *et al.*, 2004; Reid *et al.*, 2009; Jiang *et al.*, 2011; Chang *et al.*, 2014; Yin *et al.*, 2015). In the course of these studies, we have noted lack of *CHS*-silencing phenotype in the case of simultaneous silencing of *CHS* and a *PhERF2* gene encoding an ethylene response transcription factor. Given the importance of ethylene in plant responses to stress, we hypothesized that this observation might indicate an important role for this transcription factor in the antiviral RNA silencing process. The experiments reported here were designed to test this hypothesis.

Materials and methods

Plant materials and growth conditions

Petunia (*Petunia* × *hybrida*, 'Primetime Blue', or *Petunia* × *hybrida* 'Mitchell Diploid') seeds were planted in a 72-well plastic tray filled with sterile UC soil mix and germinated at room temperature with a 16/8 h day/night photoperiod. Seedlings at the 4-leaf stage were transferred to small pots for inoculation with *Agrobacterium* bearing TRV constructs, or infected with CMV, then maintained in a growth chamber at 25/20 °C day/night with a same light/dark cycle. To determine the abundance of gene transcripts in petunia plants inoculated with various TRV constructs, RNA was extracted from the inoculated leaves, the uppermost fully-expanded leaves, or from flowers at anthesis. Young leaves from petunia plants ('Mitchell Diploid') grown in a greenhouse under 25/20 °C day/night temperature and natural photoperiods were collected and used for stable transformation.

Isolation and sequence analysis of PhERF2

An 802-bp EST sequence was identified among up-regulated genes during petunia flower development from a microarray analysis (Wang *et al.*, 2013). Using this partial sequence, a further BLAST

search in the NCBI Genbank (http://blast.ncbi.nlm.nih.gov/) was carried out to identify a full-length sequence encoding an ethylener-esponsive element binding factor 2, annotated as *PhERF2*. Protein homologues of PhERF2 were identified through the BLAST search in the non-redundant GenBank protein databases. A NCBI web server (http://www.ncbi.nlm.nih.gov/Structure/cdd/wrpsb.cgi) was used to determine the conserved domain. Multiple alignments of the ERF2 proteins and phylogenic tree analysis were carried out using the ClustalW program (http://www.genome.jp/tools/clustalw/) and MEGA4 software.

Abiotic stress and hormone treatments

To examine the effects of abiotic stress and hormone treatments on the *PhERF2* expression profile, 3-week-old seedlings were used. For the salinity and drought treatments, the plants were placed in a vial with distilled water (control), water containing 100 mM NaCl, or without water at room temperature (20 °C). For the cold treatment, the seedlings were placed in a cold room at 4 °C. For the ethylene treatment, the plants were placed in a sealed glass chamber and exposed to 10 µl l^{-1} ethylene in air. For treatments with other hormones, plants were treated with solutions containing 50 µM abscisic acid (ABA), 50 µM gibberellic acid (GA_3), 200 µM salicylic acid (SA), or 200 µM methyl jasmonate (MeJA). In each case, three individual plants were collected at 0, 3, 6, 12 and 24 h post-treatment, then frozen in liquid nitrogen and stored at –80 °C.

Virus-induced gene silencing

The TRV vectors TRV1 and TRV2 have been described previously (Liu *et al.*, 2002). Our experiments were carried out with previously generated TRV-*PhPDS* or TRV-*PhCHS* constructs, in which a 138-bp *PDS* or 194-bp *CHS* fragment was cloned into the *Eco*RI or *Xba*I-*Eco*RI restriction sites in the TRV2 vector, respectively (Chen *et al.*, 2004). To create the TRV-*PhPDS* or TRV-*PhCHS* construct with a fragment of the gene of interest, *Sac*I and *Xho*I were used to digest the pDAH11 vector containing a 291-bp or 339-bp fragment of *PhERF2* or a 246-bp fragment of *PhERF3*, and the resulting product was ligated into the corresponding site in TRV-*PhPDS* or TRV-*PhCHS* (Chen *et al.*, 2004). The recombinant plasmids were transformed into *Agrobacterium tumefaciens* strain GV3101 using electroporation (Reid *et al.*, 2009; Jiang *et al.*, 2011). The *Agrobacterium* strains were cultured in 15 ml LB media (40 mg l^{-1} kanamycin, 20 mg l^{-1} gentamicin, 10 mM MES and 20 µM acetosyringone) at 28 °C in a growth chamber for 48 h. *Agrobacterium* cultures were centrifuged at 3000 *g* for 20 min, and the pelleted cells were then resuspended in infiltration buffer (10 mM $MgCl_2$, 10 mM MES and 200 µM acetosyringone) to an OD600 of 4.0. The suspensions were shaken gently at room temperature for 3–5 h before inoculation. Prior to inoculation, *Agrobacterium* cultures bearing the TRV1 and TRV2 or TRV2-derivatives were mixed together in equal volumes to a final OD600 of 2.0. A 1-ml disposal syringe was used to infiltrate the *Agrobacterium* mixture into the leaves of petunia seedlings (Reid *et al.*, 2009; Jiang *et al.*, 2011).

Semi-quantitative and real-time quantitative RT-PCR

Total RNA was extracted from the leaves and flowers of petunia plants using TRIzol reagent (Invitrogen, Carlsbad, CA, USA), and purified with RNase-free DNase I (Promega, Madison, WI, USA), according to the manufacturer's protocol. First-strand cDNA was synthesized from 2–5 µg total RNA with M-MLV reverse transcriptase (Invitrogen, Carlsbad, CA, USA). Real-time quantitative RT-PCR was carried out using the SYBR Green PCR Master Mix (2X) in an ABI7300 instrument (Applied Biosystem, Foster City, CA, USA) as previously described (Liang *et al.*, 2014). 26S ribosomal RNA served as an internal control for normalization of cDNA (Chen *et al.*, 2004; Reid *et al.*, 2009). PCR primers to sequences beyond the region of the inserted fragment for silencing were used for determination of transcript abundance of targeted genes. To confirm accumulation of TRV2 by semi-quantitative RT-PCR, two primer pairs were produced (see Supplementary Table S1 at *JXB* online), of which one (TRV2-1) covered the multiple cloning sites (MCS) in TRV2, so that the size of resulting product varied depending on the inserts in the site, whereas the other (TRV2-2), targeted the region upstream of the MCS and generated bands of uniform size (Supplementary Table S1) (Reid *et al.*, 2009).

Northern blot assay

Total RNA was isolated from the newly expanded leaves and fully open flowers of inoculated petunia plants, and low-molecular-weight RNA was precipitated using a solution of polyethylene glycol (PEG8000) and NaCl (Wang *et al.*, 2004b). Blot hybridization was carried out as previously described (Donaire *et al.*, 2008). The fragments of *PDS* (138 bps) or *CHS* (194 bps) corresponding to the silencing region were labeled with [γ-^{32}P] ATP to generate DNA probes for assessing abundance of *PDS*- or *CHS*-derived siRNAs.

Measurement of ethylene production

Leaves of petunia seedlings inoculated with TRV empty vector were harvested at different time intervals and sealed in a 50-ml plastic tube at 25 °C for 4 h. A 3-ml gas sample was taken from the tube using a gas-tight syringe, and injected into a gas chromatograph (GC-8A; Shimadzu, Kyoto, Japan) for measurement of ethylene concentration, as previously described (Chang *et al.*, 2014; Yin *et al.*, 2015).

Overexpression and RNAi silencing constructs

A 1137-bp DNA fragment containing the ORF region of the *PhERF2* was PCR-amplified using the primer pair oxPhERF2F1 and oxPhERF2R1 (see Supplementary Table S1). The amplified product was cloned into the pDAH11 vector and then transferred to a pGSA1403 vector in the forward orientation to produce the 35S::*PhERF2* construct (Chang *et al.*, 2014; Yin *et al.*, 2015). To generate the RNAi construct, primers rnaiPhERF2F1 and rnaiPhERF2R1 (Supplementary Table S1), carrying a *Spe*I-*Asc*I and a *Bam*HI-*Swa*I adaptor, respectively, were designed to amplify a 339-bp fragment. The amplified PCR products were cloned into the pDAH11 vector. The sense and antisense fragments were released from digestion of the pDAH11 plasmid and cloned into the pGSA1285 binary vector. The constructs were sequenced to confirm their fidelity as previously described (Liang *et al.*, 2014).

Stable transformation

The generated constructs were introduced into *Agrobacterium tumefaciens* strain LBA4404. The transformed bacteria were selected by incubation on an LB plate containing 25 mg l^{-1} chloramphenicol at 28 °C for 72 h. One colony was selected and cultured in YEP medium (10 g l^{-1} yeast extract, 10 g l^{-1} peptone and 5 g l^{-1} NaCl) with appropriate antibiotics for 48 h, and adjusted to an OD600 of 0.3 using sterile LB media without antibiotics. Leaves of 'Mitchell Diploid' petunias were inoculated with *Agrobacterium* and regenerated as previously described (Wang *et al.*, 2013; Liang *et al.*, 2014). Putative transgenic petunia plants were grown to flowering. The seeds were harvested and germinated in MS plates containing 100 mg l^{-1} kanamycin for selection (Estrada-Melo *et al.*, 2015; Yin *et al.*, 2015).

Inoculation assay with CMV

Cucumber mosaic virus (CMV) inoculum was obtained from leaves of Oriental hybrid lily (*Lilium*) cultivar 'Siberia'. Infectious sap was prepared by extracting CMV-infected leaves in 100 mM phosphate buffer, pH 7.0 (1:4 w/v). The fully expanded leaves of 4-week-old healthy petunia seedlings were mechanically inoculated with virus preparations as previously described (Hull, 2009). To ensure an

efficient infection, the inoculation process was carried out once more after 24 h. Subsequently, inoculated plants were maintained in the growth chamber at 22 °C for evaluation of symptoms. Transcript levels for the CMV coat protein were examined by real-time quantitative RT-PCR (Liang *et al.*, 2014; Estrada-Melo *et al.*, 2015).

Results

Identification of PhERF2

An 802-bp EST corresponding to a putative ethylene-responsive element binding factor 2 (*ERF2*) gene was identified among genes up-regulated during flower development in petunia from a microarray analysis (Wang *et al.*, 2013). A further BLAST search in the NCBI Genbank revealed a full-length mRNA sequence (accession number HQ259596, NCBI) annotated as *PhERF2* (see Supplementary Fig. S1). Analysis of the deduced polypeptide encoded by *PhERF2* using the BLAST search against non-redundant GenBank databases in the NCBI revealed homologous proteins from diverse plant species. Amino acid alignment and phylogenetic analysis showed that PhERF2 is relatively close to PhERF3 in petunia and to other proteins, such as *Solanum lycopersicum* SlJERF1 (NP_001234513), *S. tuberosum* StRAP2.12 (XP_006342909), *Prunus salicina* PsERF2a (ACM49847), *Nelumbo nucifera* NnRAP2.12 (XP_010273830), *Malus domestica* MdRAP2.12 (NP_001280975), *Nicotiana tabacum* NtCEF1 (Lee *et al.*, 2005), *Capsicum annuum* CaPF1 (Yi *et al.*, 2004) and *Arabidopsis thaliana* AtRAP2.12 (Zhao *et al.*, 2012; Ding *et al.*, 2013) (Supplementary Fig. S2).

Biotic, abiotic stresses and hormone treatments induce PhERF2 *expression*

To investigate whether transcript levels of *PhERF2* are induced by TRV infection, wild-type (WT) leaves of petunia plants at the 4-leaf stage were inoculated with *Agrobacterium* bearing an empty TRV vector. *PhERF2* transcripts increased significantly in inoculated leaves by 36 h post-inoculation (hpi) (Fig. 1A). By comparison, infection with *Agrobacterium* without the TRV plasmid (mock control) did not affect *PhERF2* transcript levels (Fig. 1A). In systemically infected upper leaves, *PhERF2* transcript abundance increased dramatically between 10 and 15 d post-inoculation (dpi), and remained high thereafter and until 25 dpi (Fig. 1B). As plant hormones and stresses play important roles in the antiviral RNA silencing processes, we examined the expression pattern of *PhERF2* in WT leaves in response to different plant growth regulator and abiotic stress treatments. The expression of *PhERF2* increased following exposure to low temperature,

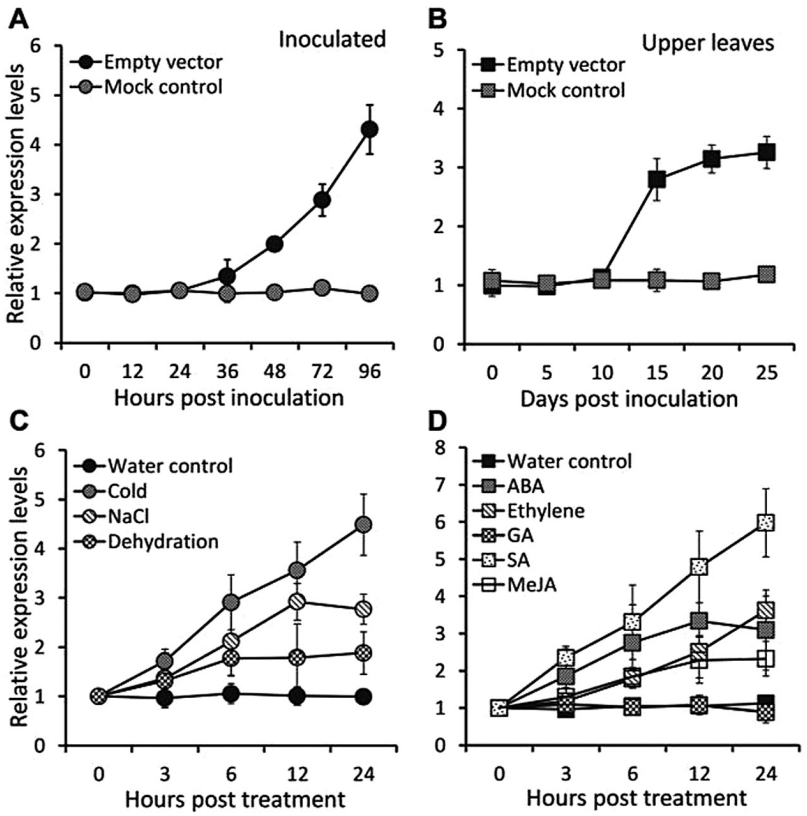

Fig. 1. Induction of *PhERF2* expression in petunia leaves infected by TRV, or treated with abiotic stresses or plant hormones. Quantitative RT-PCR analysis of *PhERF2* transcript levels in (A) inoculated and (B) systemically infected (uppermost) leaves at different time points, using 3-week-old WT seedlings infiltrated with *Agrobacterium* bearing no TRV construct (mock control) or TRV empty vector. Quantitative RT-PCR analysis of *PhERF2* transcript abundance in response to abiotic stresses (C) or plant growth regulators (D). Three-week-old WT seedlings were placed in vials with water (control), or treated with a continuous 10 μl l^{-1} ethylene, or with solutions containing either 100 mM NaCl, 50 μM ABA, 50 μM GA_3, 200 μM SA, or 200 μM MeJA, or without water (dehydration) at room temperature, or with water at 4 °C. Transcript abundances were standardized to *26S rRNA*. Error bars represent SE of the means from three biological replicates.

salt stress, and dehydration (Fig. 1C). Transcript levels of *PhERF2* also increased following treatments with SA, ABA, ethylene, and MeJA but not GA_3 (Fig. 1D).

Simultaneous silencing of PhERF2 *and* PDS *or* CHS *impairs VIGS efficiency*

VIGS has proved to be a fast and efficient method to silence genes in petunia. Therefore, to study the function of *PhERF2,* we employed a TRV-based VIGS system to silence *PhERF2* in the leaves and corollas, using *PDS* and *CHS* as visual reporters. The mock-treated and empty vector-inoculated plants showed the WT phenotype with green leaves and purple flowers (Figs 2A and 3A). In plants infected with the TRV-*PhPDS* construct, upper leaves showed a clear *PDS*-silenced photobleaching phenotype by 3 weeks post-infiltration (wpi) (Fig. 2A). The flowers on the plants infected with the TRV-*PhCHS* construct were largely white, corresponding to the silenced phenotype of *CHS* (Fig. 3A).

The plants infected with the TRV-*PhPDS*/*ERF2* or TRV-*PhCHS*/*ERF2* construct, bearing a 291-bp sequence from the 5′ end of the *PhERF2* cDNA, failed to show the normal foliar (*PDS*-photobleaching leaves) and floral (*CHS*-white flowers) silencing phenotypes (Figs 2A and 3A). These results seemed to be specific to *PhERF2*, since infection with a TRV-*PhPDS*/*ERF3* or TRV-*PhCHS*/*ERF3* construct bearing a 246-bp fragment of *PhERF3*, a paralog of *PhERF2* (see Supplementary Fig. S2B), produced the normal silencing phenotypes in leaves and flowers (Figs 2A and 3A). Moreover, infection with a TRV-*PhPDS*/*ERF2* or TRV-*PhCHS*/*ERF2* vector bearing a different 339-bp fragment (Fragment 2) from the 3′ region of the *PhERF2* cDNA also failed to elicit the silencing phenotypes (Figs 2A and 3A).

VIGS silencing of PhERF2 *does not suppress TRV movement or replication*

To understand why upper leaves of plants infected with TRV-*PhPDS*/*ERF2* displayed none of the photobleaching seen in those from plants infected with TRV-*PhPDS* and TRV-*PhPDS*/*ERF3* (Fig. 2A), we performed semi-quantitative and real-time quantitative RT-PCR to analyse transcript abundances of genes including *PhERF2*, *PDS*, *CHS*, TRV RNA1, and RNA2. The results revealed a 50% reduction of *PhERF2* transcript levels in leaves from TRV-*PhPDS*/*ERF2*-infected plants, and 2-fold increases in transcripts in leaves from TRV-*PhPDS*- and TRV-*PhPDS*/*ERF3*-infected plants, compared to the mock control (Fig. 2B, C). *PDS* transcript abundance negatively correlated with the photobleaching in the upper leaves (Fig. 2C). Abundance of *PDS* transcript in the TRV-*PhPDS*- and TRV-*PhPDS*/*ERF3*-infected plants was reduced by over 90% whereas *PDS* abundance was only 20% less than the controls in the TRV-*PhPDS*/*ERF2*-infected plants (Fig. 2C). Accumulation of TRV RNA1 (TRV1) and RNA2 (TRV2) in the leaves of plants agro-infiltrated with an empty vector or TRV-*PhPDS*/*ERF2* constructs was significantly higher than in those of TRV-*PhPDS*- and TRV-*PhPDS*/*ERF3*-infected plants (Fig. 2B, C). Similar results were obtained when petunia plants were infected with the TRV-*PhCHS*/*ERF2* construct using a flower-specific visual reporter (*CHS*) (Fig. 3A–C).

VIGS Silencing of PhERF2 *affects expression of RNA silencing-related genes*

To study the role of *PhERF2* in the RNA silencing process, we determined transcript abundances of a number of putative RNA silencing-related genes. Infection with TRV empty vector or silencing constructs resulted in changes in expression of *RDR*s (*RDR1*, *2*, *6*), *DCL*s (*DCL1–4*) and *AGO*s (*AGO1*, *2*, *4*) (Fig. 2D). Almost all the selected genes were up-regulated by infection with the TRV empty vector compared to the mock control (Fig. 2D). Up-regulation was considerably higher for *RDR2*, *DCL2*, and *AGO2* in leaves of plants showing the *PDS*-silenced photobleaching phenotype (TRV-*PhPDS* and TRV-*PhPDS*/*ERF3*) (Fig. 2D). However, this increase was not observed in leaves from TRV-*PhPDS*/*ERF2*-infected plants, in which *RDR6* expression levels were also significantly lower than in photobleached leaves (Fig. 2D).

Using the *PDS* silencing insert as a labeled probe for hybridization, we conducted northern blot analysis to visualize the abundance of TRV-*PhPDS*-derived siRNAs. Leaves from TRV-*PhPDS*- and TRV-*PhPDS*/*ERF3*-infected plants contained a 22-nt RNA fragment that bound to the labeled probe (Fig. 2E). But there was no detectable signal in leaves from TRV-*PhPDS*/*ERF2*-infected plants (Fig. 2E). Similar patterns from the RNA silencing-related gene expression and northern blot analyses were obtained using corollas of petunia plants inoculated with TRV-*PhCHS*-based constructs (Fig. 3D, E).

PhERF2-*RNAi silencing impairs VIGS efficiency*

To further study the function of *PhERF2*, we generated *PhERF2*-RNAi lines in petunia. Growth and development of *PhERF2*-RNAi lines was substantially slower than WT plants (Fig. 4A). The *PhERF2*-RNAi lines (#1 and #4) showed substantial reduction in *PhERF2* transcript abundance (Fig. 4B). The transcript abundance of RNA silencing-related genes, including *RDR2*, *RDR6*, *DCL2*, and *AGO2*, was also significantly lower in these RNAi-silencing lines (Fig. 4C). When these lines were infected with the TRV-*PhPDS* silencing construct, they showed no, or much reduced, photobleaching (Fig. 4D), and a concomitant high abundance of *PDS*, TRV RNA1, and RNA2 transcripts in comparison to the photobleached leaves of infected WT plants (Fig. 4E).

Overexpression of PhERF2 *enhances silencing*

To further investigate the role of *PhERF2* in the antiviral RNA silencing process, we also generated *PhERF2* overexpression lines in petunia. Transgenic plants overexpressing *PhERF2* under the control of the *Cauliflower mosaic virus* (CaMV) 35S promoter grew faster (Fig. 5A), and had up to six times the *PhERF2* transcript abundance found in WT plants (Fig. 5B). Transcripts of the RNA silencing-related

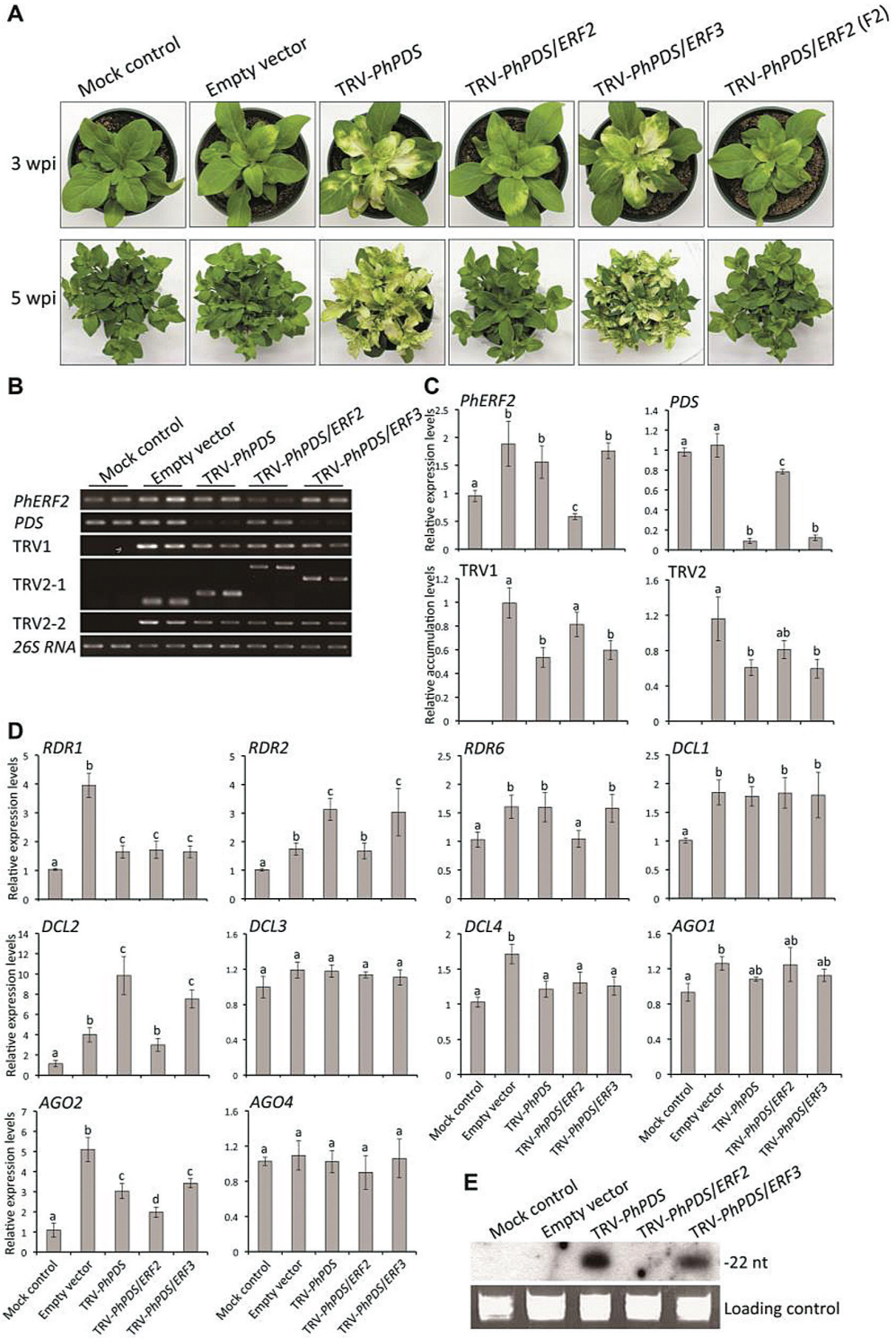

Fig. 2. Failed development of photobleaching phenotype in the leaves of VIGS-silenced *PhERF2* plants using *PDS* as a visual reporter. (A) Representative phenotypes of WT plants 3 and 5 weeks post-inoculation (wpi) with non-transformed *Agrobacterium* (mock control), or *Agrobacterium* bearing a TRV empty vector, TRV-*PhPDS*, TRV-*PhPDS*/*ERF2*, TRV-*PhPDS*/*ERF3*, and TRV-*PhPDS*/*ERF2* (fragment 2, F2) constructs. (B), (C) Semi-quantitative and quantitative RT-PCR analysis of transcript abundances for *PhERF2*, *PDS*, TRV RNA1 (TRV1), and TRV RNA2 (TRV2-1, -2) in uppermost younger leaves of plants 3 wpi. Primers for TRV2-1 were designed from the region outside the multiple cloning site (MCS) in the vector and produced variable sizes of products depending on the presence of the *PhPDS*, *PhPDS*/*ERF2*, and *PhPDS*/*ERF3* inserts in the TRV2 vector. Primers for TRV2-2 were used to produce the same sizes of products from the TRV2 vector. Relative accumulation levels were normalized to *26S rRNA*. Error bars represent SE of the means from three biological replicates. Different letters indicate statistical significance as calculated by Duncan's multiple range test at $P<0.05$. (D) Quantitative RT-PCR analysis of transcript abundances for RNA silencing-related genes, including *RDR1*, *RDR2*, *RDR6*, *DCL1*, *DCL2*, *DCL3*, *DCL4*, *AGO1*, *AGO2*, and *AGO4*, in uppermost younger leaves of plants at 3 wpi. Abundance of *26S rRNA* was used as an internal control. Error bars represent SE of the means from three biological replicates. Different letters denote statistical significance using Duncan's multiple range test at $P<0.05$. (E) Northern-blot analysis of *PDS* insert-derived siRNA levels in topmost younger leaves of plants at 3 wpi. ^{32}P-labeled oligonucleotide probes corresponding to the *PDS* insert sequence were used for detection. Ethidium bromide-stained *5S rRNA* served as a loading control.

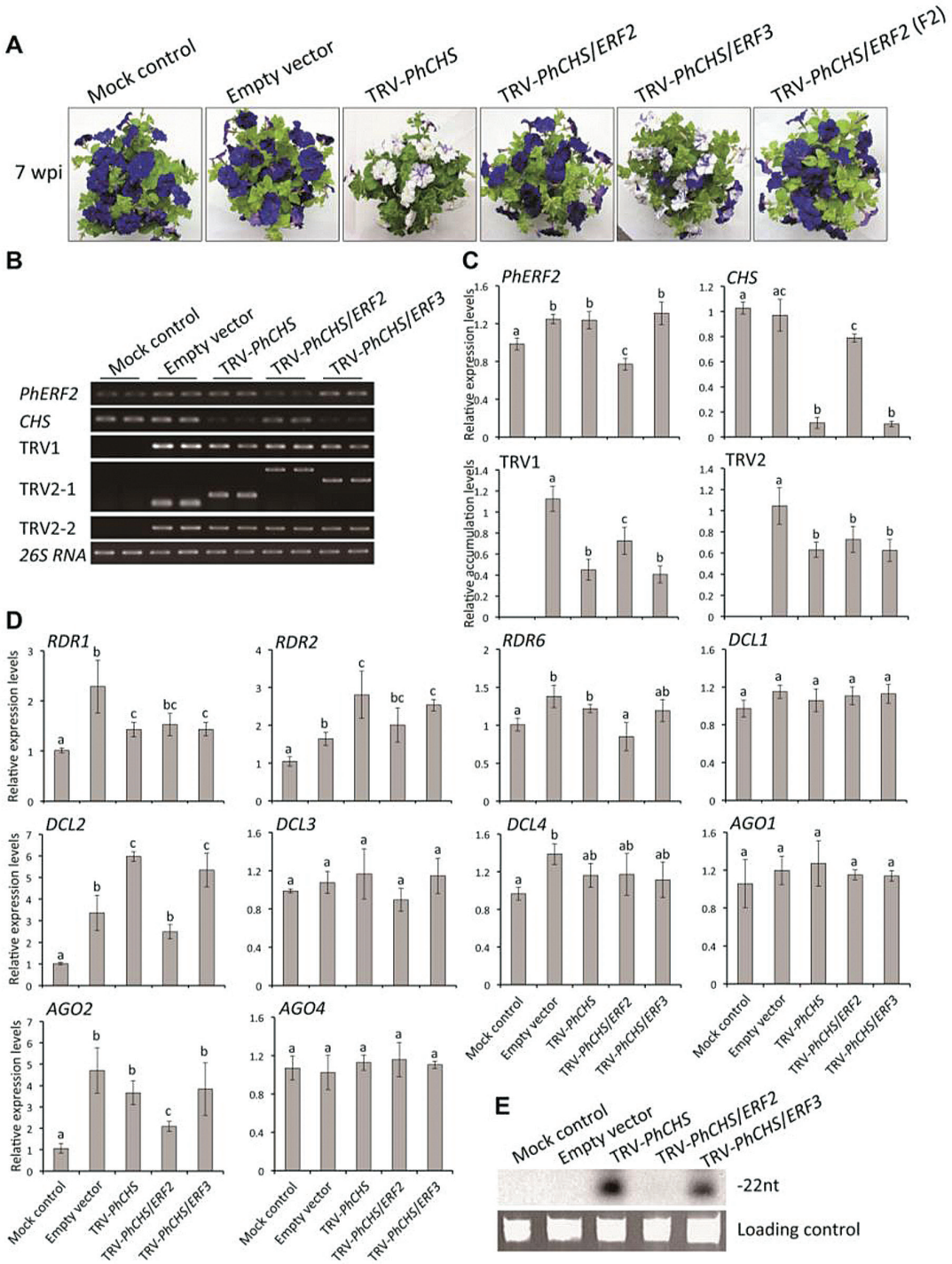

Fig. 3. Failed development of the white-corollas phenotype in the flowers of VIGS-silenced *PhERF2* plants using *CHS* as a visual reporter. (A) Representative phenotypes of WT plants 7 weeks post-inoculation (wpi) with non-transformed *Agrobacterium* (mock control), or *Agrobacterium* bearing the TRV empty vector, TRV-*PhCHS*, TRV-*PhCHS/ERF2*, TRV-*PhCHS/ERF3*, and TRV-*PhCHS/ERF2* (fragment 2, F2) constructs. (B), (C) Semi-quantitative and quantitative RT-PCR analysis of transcript abundances for *CHS*, *PhERF2*, TRV RNA1 (TRV1), and TRV RNA2 (TRV2-1, -2) in the corollas. Flowers were harvested at anthesis 7 wpi. Primers for TRV2-1 were designed from the region outside the multiple cloning site (MCS) in the vector and produced variable sizes of products depending on the presence of the *PhCHS*, *PhCHS/ERF2*, and *PhCHS/ERF3* inserts in the TRV2 vector. Primers for TRV2-2 were used for quantitative RT-PCR to produce the same sizes of products from the TRV2 vector. Abundance of *26S rRNA* was used as an internal control. SE of the means from three biological replicates are indicated by the error bars. Different letters denote statistical significance using Duncan's multiple range test at $P<0.05$. (D) Quantitative RT-PCR analysis of transcript abundances for RNA silencing-related genes, including *RDR1*, *RDR2*, *RDR6*, *DCL1*, *DCL2*, *DCL3*, *DCL4*, *AGO1*, *AGO2*, and *AGO4*, in the corollas. Flowers were harvested at anthesis 7 wpi. Abundance of *26S rRNA* was used as an internal control. Error bars represent the SE of the means from three biological replicates. Different letters denote statistical significance using Duncan's multiple range test at $P<0.05$. (E) Northern-blot analysis of *CHS* insert-derived siRNA levels in the corollas, harvested at anthesis, of plants at 7 wpi. ^{32}P-labeled oligonucleotide probes corresponding to *CHS* insert sequence were used for detection. Ethidium bromide-stained *5S rRNA* was served as a loading control.

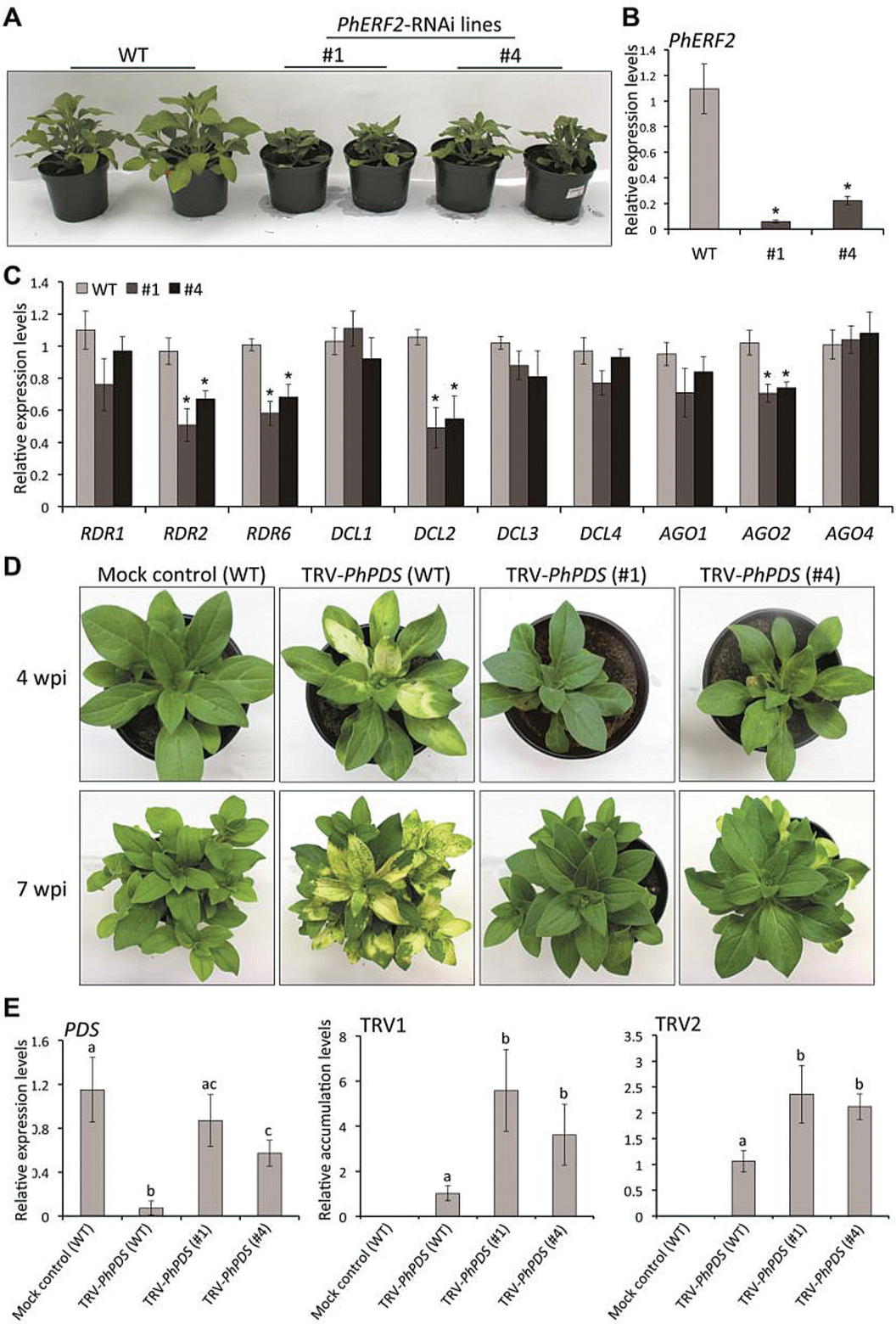

Fig. 4. Impairment of photobleaching phenotype in *PhERF2*- RNAi lines inoculated with *Agrobacterium* bearing TRV-*PhPDS*. (A) Representative growth phenotypes of WT and *PhERF2*-RNAi lines (#1 and #4) 40 d post-germination. Note that *PhERF2*-RNAi lines showed delayed growth. (B), (C) Quantitative RT-PCR analysis of transcript abundances for *PhERF2, RDR1*, *RDR2*, *RDR6*, *DCL1*, *DCL2*, *DCL3*, *DCL4*, *AGO1*, *AGO2*, and *AGO4* in the leaves of WT and *PhERF2*-RNAi lines (#1 and #4). Uppermost leaves of 4-week-old plants were used. (D) Representative phenotypes of WT and *PhERF2*-RNAi lines (#1 and #4) inoculated with *Agrobacterium* bearing no TRV vector (mock control) or a TRV-*PhPDS* construct at 4 and 7 weeks post-inoculation. (E) Quantitative RT-PCR analysis of transcript abundances for *PDS*, TRV RNA1 (TRV1), and TRV RNA2 (TRV2) in uppermost leaves of WT and *PhERF2*-RNAi lines (#1 and #4) inoculated with *Agrobacterium* bearing no TRV vector (mock control) or a TRV-*PhPDS* construct. Transcript abundances were standardized to *26S rRNA*. Error bars represent the SE of the means from three biological replicates (B, C, E). Asterisks (B, C) or different letters (E) denote statistical significance using Duncan's multiple range test at $P<0.05$.

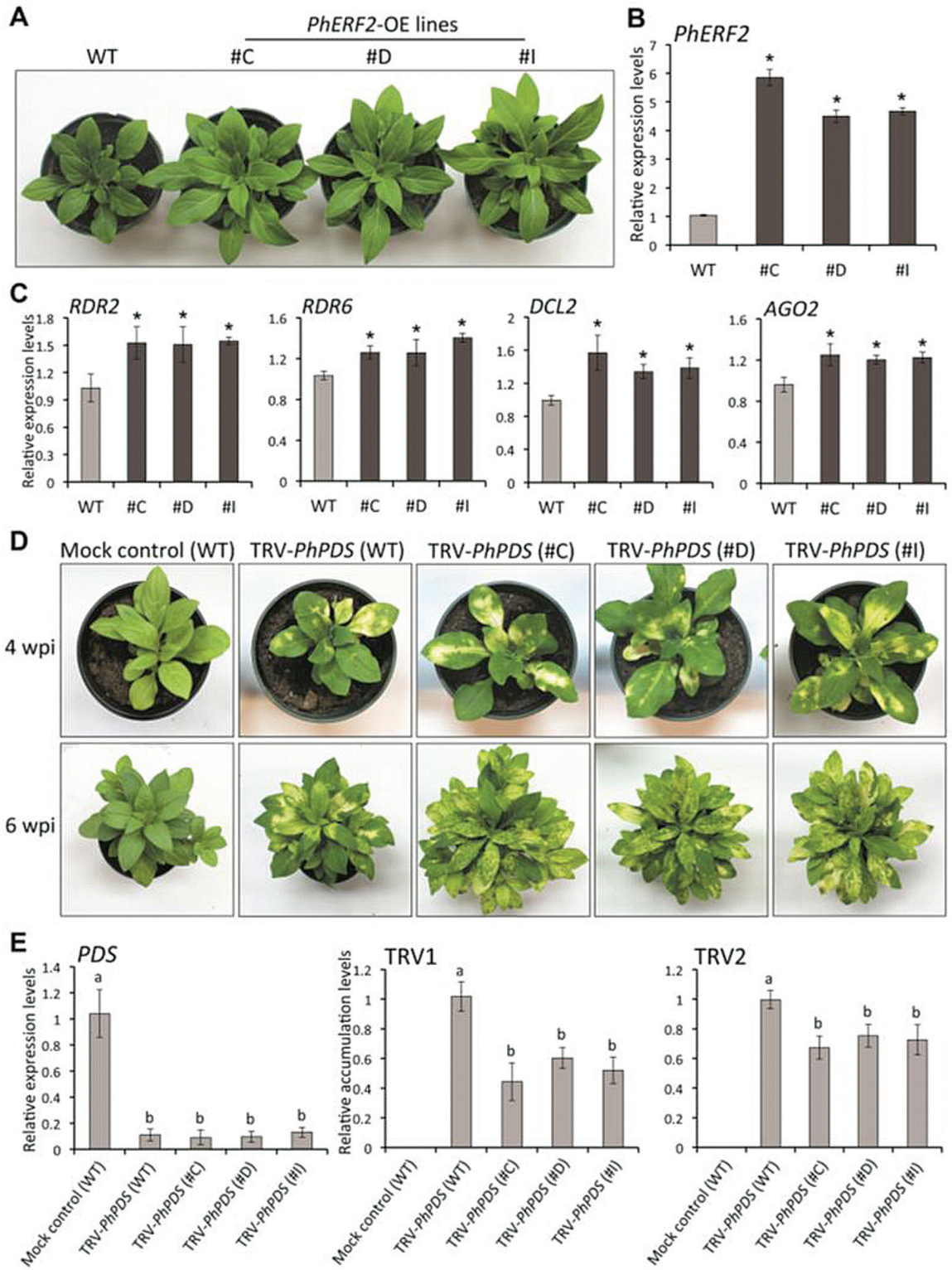

Fig. 5. Photobleaching phenotypes of *PhERF2*-overexpressing lines inoculated with *Agrobacterium* bearing a TRV-*PhPDS* construct. (A) Representative growth phenotypes of WT and *PhERF2*-overexpressing (OE) lines (#C, #D and #I) 30 d post-germination. Note that overexpression of *PhERF2* enhanced plant growth. (B), (C) Quantitative RT-PCR analysis of transcript abundances for *PhERF2, RDR2*, *RDR6*, *DCL2*, and *AGO2* in the leaves of WT and *PhERF2*-OE plants (#C, #D and #I). Samples were harvested from uppermost leaves of 4-week-old plants. (D) Representative phenotypes of WT and *PhERF2*-OE lines (#C, #D and #I) inoculated with *Agrobacterium* bearing no TRV vector (mock control) or a TRV-*PhPDS* construct at 4 and 6 weeks post-inoculation (wpi). (E) Quantitative RT-PCR analysis of transcript abundances for *PDS* and TRV RNA1 (TRV1), and TRV RNA2 (TRV2) in uppermost leaves of WT and *PhERF2*-OE lines (#C, #D and #I) inoculated with *Agrobacterium* bearing no TRV vector (mock control) or a TRV-*PhPDS* construct at 4 wpi. Abundance of *26S rRNA* was used as an internal control. Error bars represent the SE of the means from three biological replicates (B, C, E). Asterisks (B, C) or different letters (E) denote statistical significance using Duncan's multiple range test at $P<0.05$.

genes including *RDR2*, *RDR6*, *DCL2*, and *AGO2* were significantly higher in the overexpressing lines than in the WT controls (Fig. 5C). When infected with the TRV-*PhPDS* silencing construct, the *PhERF2*-overexpressing lines showed similar silencing phenotypes and reduction in *PDS* transcripts to those seen in TRV-*PhPDS*-inoculated WT plants (Fig. 5D, E). The accumulation of TRV RNA1 and RNA2 was lower in the overexpressing lines than in the WT when inoculated with TRV-*PhPDS* construct (Fig. 5E).

PhERF2 *affects disease susceptibility*

Given that *PhERF2* is an important factor in antiviral RNA silencing against TRV, the role of *PhERF2* in response to *Cucumber mosaic virus* (CMV) was then examined. *PhERF2*-RNAi lines inoculated with CMV showed more distortion and yellow mottling of systemically infected leaves than WT plants (Fig. 6A). In contrast, infected *PhERF2*-overexpressing lines had much milder symptoms and continued growth (Fig. 6A). These phenotypes were correlated with measured accumulations of CMV coat protein (*CP*) transcripts, which were significantly higher in *PhERF2*-RNAi lines and dramatically lower in *PhERF2*-overexpressing lines than in WT plants (Fig. 6B).

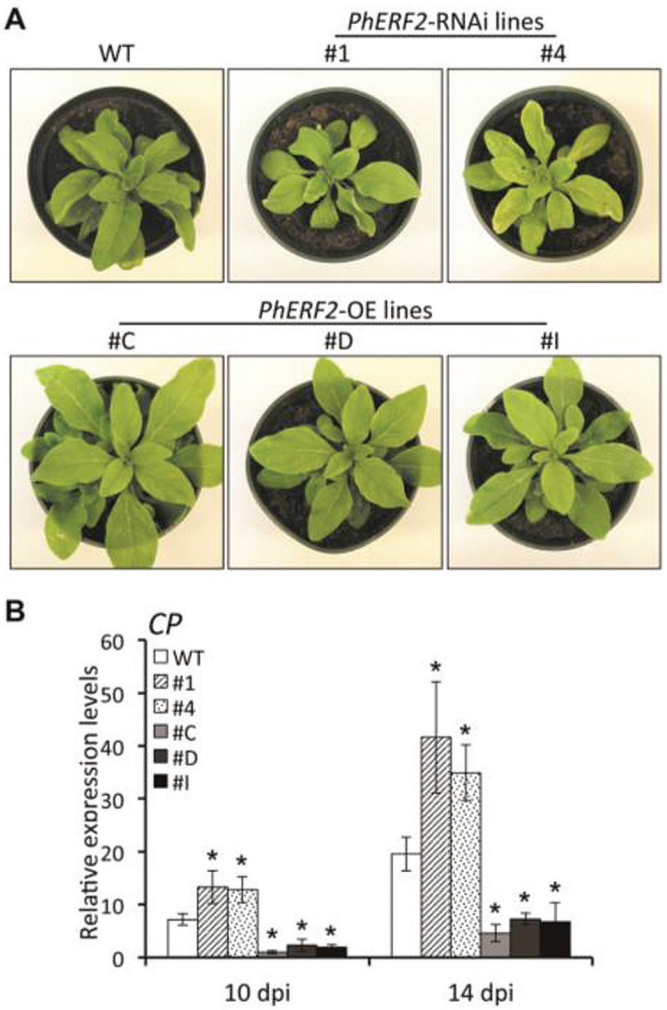

Fig. 6. Involvement of PhERF2 in the defense of petunia plants against CMV. (A) Disease symptoms of WT, *PhERF2*-RNAi (#1 and #4), and *PhERF2*-overexpressing (OE) (#C, #D and #I) lines inoculated with CMV at 2 weeks post-inoculation; 4-week-old seedlings were used for inoculation. (B) Quantitative RT-PCR analysis of CMV coat protein (*CP*) transcript abundances in systemically infected (uppermost) leaves of WT, *PhERF2*-RNAi (#1 and #4), and *PhERF2*-OE (#C, #D and #I) lines at 10 and 14 d post-inoculation. Transcript abundances were standardized to *26S rRNA*. Error bars represent the SE of the means from three biological replicates. Asterisks denote statistical significance using Duncan's multiple range test at $P<0.05$.

Discussion

The data presented here support our hypothesis that the ethylene-responsive element binding factor PhERF2 plays an important role in antiviral RNA silencing (see Supplementary Fig. S3). ERFs belong to the plant-specific AP2/ERF transcription factor superfamily, whose members share a highly conserved AP2/ERF DNA binding domain with a length of 57–66 amino acids (Okamuro *et al.*, 1997). In Arabidopsis, there are a total of 122 putative ERF genes (Nakano *et al.*, 2006). They appear to bind to a *cis*-acting GCC box with a core AGCCGCC motif (Hao *et al.*, 1998) that is commonly found in the promoter region of defense-related genes downstream from the ethylene signaling pathway (Ohme-Takagi and Shinshi, 1995).

Ethylene is the key regulator in the senescence of petunia flowers, and we have been dissecting the control of the process by silencing structural and regulatory genes, including *ERF* genes, in the ethylene response cascade (Wang *et al.*, 2013; Chang *et al.*, 2014; Yin *et al.*, 2015). When we silenced *PhERF2*, using a TRV vector containing a fragment of *PhERF2* and either a foliar or floral reporter gene (*PDS* or *CHS*, respectively), we noted a dramatic reduction in VIGS efficiency, as demonstrated by very little photobleaching in the leaves or white corollas on the normally purple flowers (Figs 2A and 3A). *PhERF2* transcripts were abundant in control plants infected with the empty TRV vector. These findings led to the hypothesis that *PhERF2* might play an important role in the transcriptional regulation of the silencing response system.

Antiviral RNA silencing involves up-regulation of a number of genes, including *RDR*s, *DCL*s, and *AGO*s, that are required for the generation and cleavage of double-stranded RNA (dsRNA) and its processing into virus-derived small interfering RNAs (vsiRNA). In Arabidopsis, four DCLs, six RDRs and ten AGOs serve as critical components of the silencing machinery (Donaire *et al.*, 2008; Zhang *et al.*, 2012). DCL2, DCL3, and DCL4 catalyse the cleavage of exogenous RNAs with double-stranded features into 22-, 24- and 21-nt siRNAs, respectively (Dunoyer *et al.*, 2005; Donaire *et al.*, 2008; Axtell, 2013).

We found that the silencing efficiency of both *PDS* and *CHS* reporters affected by silencing or overexpression of *PhERF2* was associated with substantial changes in abundance of silencing-associated genes, including *RDR2*, *RDR6*, *DCL2*, and *AGO2*. It appears likely that *PhERF2* modifies the transcription of these genes by binding *cis*-elements in their promoters. This possibility requires further examination in the future.

Many researchers have examined the effects of modulating expression of genes in the silencing complex on disease resistance. In *Nicotiana benthamiana*, for example, RDR6 was shown to be critical in resistance to CMV (Mourrain *et al.*, 2000) and *Potato virus X* (PVX) (Schwach *et al.*, 2005). In Arabidopsis, *DCL* mutants accumulate higher titers of TCV and CMV (Bouché *et al.*, 2006), TRV (Donaire *et al.*, 2008), *Turnip mosaic virus* (TuMV) (Garcia-Ruiz *et al.*, 2010), and *Tobacco mosaic virus* (TMV) (Lewsey and Carr, 2009). Our observations of increased and reduced TRV accumulations in *PhERF2*-silenced (Fig. 4E) and -overexpressing (Fig. 5E) petunias, respectively, and of the negative correlation between *PhERF2* expression and susceptibility to CMV (Fig. 6) are consistent with these findings, and support the hypothesis that *PhERF2* plays a regulatory role in the antiviral RNA silencing process. Mutants of *RAP2.2*, the Arabidopsis homolog of *PhERF2*, showed increased susceptibility to *Botrytis cinerea*, while its overexpression resulted in enhanced resistance to this pathogen (Zhao *et al.*, 2012). It seems possible that *PhERF2* might be involved in a general response to disease pressure, and future studies will examine the effect of up- and down-regulation of this transcription factor on susceptibility to fungal pathogens.

We were particularly interested in the roles of *PhERF2* and ethylene in plant growth and development and stress responses. Expression analysis demonstrated that *PhERF2* was also up-regulated in plants treated with the hormones SA, ABA, ethylene, and MeJA. These regulators sometimes function as growth inhibitors, and the interplay between *PhERF2* and these regulators may explain the substantial reduction in growth rate that was observed in silenced petunias (Fig. 4A) or the improvement of plant growth in the overexpressing lines (Fig. 5A). Although petunia corollas are ethylene sensitive (Reid and Wu, 1992), there was no significant change in flower longevity in transgenic plants where *PhERF2* was silenced or overexpressed (see Supplementary Table S2). Presumably *PhERF2* is not involved in ethylene-triggered floral senescence. We did, however, find that abiotic factors, such as cold, salt, and drought, enhanced the levels of *PhERF2* (Fig. 1C). This is consistent with studies on *PhERF2* homologs in other species. *NtCEF1* from tobacco is induced by cold and salt (Lee *et al.*, 2005). Salt treatment increases mRNA levels of *JERF1* (Zhang *et al.*, 2004) and *JERF3* (Wang *et al.*, 2004a) in tobacco, and plants overexpressing these genes were more tolerant of salt stress. *CaPF1* in pepper is rapidly and strongly activated under cold and salt conditions, and upregulation of this gene confers freezing tolerance (Yi *et al.*, 2004). Future work will include a study of the response of silenced and overexpressing plants to a range of abiotic stresses.

Our results suggest that *PhERF2* plays an important role in antiviral RNA silencing. The identification of PhERF2 as a positive regulator in the TRV-based VIGS system may provide a valuable solution to enhance the VIGS response when silencing efficiency is low, as has been observed in some species in which the TRV-based VIGS system has been tested (e.g. woody species) (Shen *et al.*, 2015). Thus it may be possible to transiently overexpress the PhERF2 or homologous proteins simultaneously or prior to the inoculation of silencing vectors. Or the inoculated plants could also be treated with ethylene or SA to increase the endogenous *ERF2*-like expression, which may lead to enhancement of the silencing efficiency. It is also worth mentioning that enhanced *PhERF2* expression by low temperature may lead to improvement of gene silencing efficiency in VIGS systems. This notion is supported by the fact that gene silencing efficiency is enhanced by low temperature with a TRV-based VIGS system in tomato (Fu *et al.*, 2006) and with a geminivirus-mediated VIGS system in cotton plants (Tuttle *et al.*, 2008). It would also be interesting in the future to examine whether PhERF2 plays any positive roles in other VIGS systems.

Supplementary data

Supplementary data are available at *JXB* online.

Figure S1. Complete sequence of petunia *PhERF2* cDNA.

Figure S2. Amino acid sequence analysis of petunia PhERF2.

Figure S3. A proposed model for the roles of PhERF2 in antiviral RNA silencing.

Table S1. Primers used for semi-quantitative and real-time quantitative RT-PCR.

Table S2. The longevity of attached flowers from WT, *PhERF2*-RNAi and -overexpressing plants.

Acknowledgements

We thank Dr Bryce Falk for technical assistance in the northern blot analysis and Xiaoqing Xie for help in the transformation experiments. Dr Weixing Shan kindly hosted some of the experiments in his laboratory. We appreciate Lee Ann Richmond's assistance with the analytical instrumentation. This work was partially supported by United States Department of Agriculture (USDA) CRIS project 5306-21000-019-00D.

References

Axtell MJ. 2013. Classification and comparison of small RNAs from plants. Annual Review of Plant Biology **64,** 137–159.

Baumberger N, Baulcombe D. 2005. *Arabidopsis* argonaute1 is an RNA slicer that selectively recruits microRNAs and short interfering RNAs. Proceedings of the National Academy of Sciences, USA **102,** 11928–11933.

Bouché N, Lauressergues D, Gasciolli V, Vaucheret H. 2006. An antagonistic function for *Arabidopsis* DCL2 in development and a new function for DCL4 in generating viral siRNAs. The EMBO Journal **25,** 3347–3356.

Broderick SR, Jones ML. 2014. An optimized protocol to increase virus-induced gene silencing efficiency and minimize viral symptoms in petunia. Plant Molecular Biology Reporter **32,** 219–233.

Burch-Smith TM, Schiff M, Liu Y, Dinesh-Kumar SP. 2006. Efficient virus-induced gene silencing in *Arabidopsis*. Plant Physiology **142,** 21–27.

Chang X, Donnelly L, Sun D, Rao J, Reid MS, Jiang CZ. 2014. A petunia homeodomain-leucine zipper protein, PhHD-Zip, plays an important role in flower senescence. PLoS One **9,** e88320.

Chen JC, Jiang CZ, Gookin T, Hunter D, Clark D, Reid MS. 2004. Chalcone synthase as a reporter in virus-induced gene silencing studies of flower senescence. Plant Molecular Biology **55,** 521–530.

Deleris A, Gallego-Bartolome J, Bao J, Kasschau KD, Carrington JC, Voinnet O. 2006. Hierarchical action and inhibition of plant dicer-like proteins in antiviral defense. Science **313,** 68–71.

Di Stilio VS, Kumar RA, Oddone AM, Tolkin TR, Salles P, McCarty K. 2010. Virus-induced gene silencing as a tool for comparative functional studies in *Thalictrum*. PLoS One **5,** e12064.

Dinesh-Kumar S, Anandalakshmi R, Marathe R, Schiff M, Liu Y. 2003. Virus-induced gene silencing. Methods in Molecular Biology **236,** 287–293.

Ding Y, Liu N, Virlouvet L, Riethoven JJ, Fromm M, Avramova Z. 2013. Four distinct types of dehydration stress memory genes in *Arabidopsis thaliana*. BMC Plant Biology **13,** 229.

Donaire L, Barajas D, Martínez-García B, Martínez-Priego L, Pagán I, Llave C. 2008. Structural and genetic requirements for the biogenesis of *Tobacco rattle virus*-derived small interfering RNAs. Journal of Virology **82,** 5167–5177.

Dunoyer P, Himber C, Voinnet O. 2005. Dicer-like 4 is required for RNA interference and produces the 21-nucleotide small interfering RNA component of the plant cell-to-cell silencing signal. Nature Genetics **37,** 1356–1360.

Estrada-Melo AC, Chao, Reid MS, Jiang CZ. 2015. Overexpression of an ABA biosynthesis gene using a stress-inducible promoter enhances drought resistance in petunia. Horticulture Research **2,** 15013.

Fragkostefanakis S, Sedeek KEM, Raad M, Zaki MS, Kalaitzis P. 2014. Virus induced gene silencing of three putative prolyl 4-hydroxylases enhances plant growth in tomato (*Solanum lycopersicum*). Plant Molecular Biology **85,** 459–471.

Fu DQ, Zhu BZ, Zhu HL, Jiang WB, Luo YB. 2005. Virus-induced gene silencing in tomato fruit. The Plant Journal **43,** 299–308.

Fu DQ, Zhu B, Zhu H, Zhang H, Xie Y, Jiang W, Zhao X, Luo Y. 2006. Enhancement of virus-induced gene silencing in tomato by low temperature and low humidity. Molecules and Cells **21,** 153–160.

Garcia-Ruiz H, Takeda A, Chapman EJ, Sullivan CM, Fahlgren N, Brempelis KJ, Carrington JC. 2010. *Arabidopsis* RNA-dependent RNA polymerases and dicer-like proteins in antiviral defense and small interfering RNA biogenesis during *Turnip mosaic virus* infection. The Plant Cell **22,** 481–496.

Gould B, Kramer EM. 2007. Virus-induced gene silencing as a tool for functional analyses in the emerging model plant *Aquilegia* (columbine, Ranunculaceae). Plant Methods **3,** 6.

Hao D, Ohme-Takagi M, Sarai A. 1998. Unique mode of GCC box recognition by the DNA-binding domain of ethylene-responsive element-binding factor (ERF domain) in plant. Journal of Biological Chemistry **273,** 26857–26861.

Hull R. 2009. Mechanical inoculation of plant viruses. Current Protocols in Microbiology , 16B.16.11–16B.16.14.

Jaubert M, Bhattacharjee S, Mello AF, Perry KL, Moffett P. 2011. Argonaute2 mediates RNA-silencing antiviral defenses against *Potato virus X* in *Arabidopsis*. Plant Physiology **156,** 1556–1564.

Jiang CZ, Chen JC, Reid MS. 2011. Virus-induced gene silencing in ornamental plants. In Kodama H, Komamin A, eds. *RNAi and plant gene function analysis* . Springer, 81–96.

Jiang CZ, Lu F, Imsabai W, Meir S, Reid MS. 2008. Silencing polygalacturonase expression inhibits tomato petiole abscission. Journal of Experimental Botany **59,** 973–979.

Jones L, Keining T, Eamens A, Vaistij FE. 2006. Virus-induced gene silencing of argonaute genes in *Nicotiana benthamiana* demonstrates that extensive systemic silencing requires argonaute1-like and argonaute4-like genes. Plant Physiology **141,** 598–606.

Kumagai M, Donson J, Della-Cioppa G, Harvey D, Hanley K, Grill L. 1995. Cytoplasmic inhibition of carotenoid biosynthesis with virus-derived RNA. Proceedings of the National Academy of Sciences, USA **92,** 1679–1683.

Lee JH, Kim DM, Lee JH, Kim J, Bang JW, Kim WT, Pai HS. 2005. Functional characterization of NtCEF1, an AP2/EREBP-type transcriptional activator highly expressed in tobacco callus. Planta **222,** 211–224.

Lewsey MG, Carr JP. 2009. Effects of dicer-like proteins 2, 3 and 4 on *Cucumber mosaic virus* and *Tobacco mosaic virus* infections in salicylic acid-treated plants. Journal of General Virology **90,** 3010–3014.

Liang YC, Reid MS, Jiang CZ. 2014. Controlling plant architecture by manipulation of gibberellic acid signalling in petunia. Horticulture Research **1,** 14061.

Liu Y, Schiff M, Dinesh-Kumar S. 2002. Virus-induced gene silencing in tomato. The Plant Journal **31,** 777–786.

Lukhovitskaya NI, Solovieva AD, Boddeti SK, Thaduri S, Solovyev AG, Savenkov EI. 2013. An RNA virus-encoded zinc-finger protein acts as a plant transcription factor and induces a regulator of cell size and proliferation in two tobacco species. The Plant Cell **25,** 960–973.

Mourrain P, Béclin C, Elmayan T, Feuerbach F, Godon C, Morel JB, Jouette D, Lacombe AM, Nikic S, Picault N. 2000. *Arabidopsis* SGS2 and SGS3 genes are required for post-transcriptional gene silencing and natural virus resistance. Cell **101,** 533–542.

Nakano T, Suzuki K, Fujimura T, Shinshi H. 2006. Genome-wide analysis of the ERF gene family in *Arabidopsis* and rice. Plant Physiology **140,** 411–432.

Ohme-Takagi M, Shinshi H. 1995. Ethylene-inducible DNA binding proteins that interact with an ethylene-responsive element. The Plant Cell **7,** 173–182.

Okamuro JK, Caster B, Villarroel R, Van Montagu M, Jofuku KD. 1997. The AP2 domain of APETALA2 defines a large new family of DNA binding proteins in *Arabidopsis*. Proceedings of the National Academy of Sciences, USA **94,** 7076–7081.

Peterson RB, Eichelmann H, Oja V, Laisk A, Talts E, Schultes NP. 2013. Functional aspects of silencing and transient expression of psbS in *Nicotiana benthamiana*. American Journal of Plant Sciences **4,** 1521–1532.

Reid MS, Chen JC, Jiang CZ. 2009. Virus-induced gene silencing for functional characterization of genes in petunia. In: Gerats T, Strommer J. eds. *Petunia* . Springer, 381–394.

Reid MS, Wu MJ. 1992. Ethylene and flower senescence. Plant Growth Regulation **11,** 37–43.

Scholthof HB, Alvarado VY, Vega-Arreguin JC, Ciomperlik J, Odokonyero D, Brosseau C, Jaubert M, Zamora A, Moffett P. 2011. Identification of an argonaute for antiviral RNA silencing in *Nicotiana benthamiana*. Plant Physiology **156,** 1548–1555.

Schwach F, Vaistij FE, Jones L, Baulcombe DC. 2005. An RNA-dependent RNA polymerase prevents meristem invasion by *Potato virus X* and is required for the activity but not the production of a systemic silencing signal. Plant Physiology **138,** 1842–1852.

Senthil-Kumar M, Mysore KS. 2011. Virus-induced gene silencing can persist for more than 2 years and also be transmitted to progeny seedlings in *Nicotiana benthamiana* and tomato. Plant Biotechnology Journal **9,** 797–806.

Shen Z, Sun J, Yao J, Wang S, Ding M, Zhang H, Qian Z, Zhao N, Sa G, Zhao R. 2015. High rates of virus-induced gene silencing by *Tobacco rattle virus* in *Populus*. Tree Physiology **35,** 1016–1029.

Spitzer B, Zvi MMB, Ovadis M, Marhevka E, Barkai O, Edelbaum O, Marton I, Masci T, Alon M, Morin S. 2007. Reverse genetics of floral scent: application of *Tobacco rattle virus*-based gene silencing in petunia. Plant Physiology **145,** 1241–1250.

Szittya G, Silhavy D, Molnár A, Havelda Z, Lovas Á, Lakatos L, Bánfalvi Z, Burgyán J. 2003. Low temperature inhibits RNA silencing-mediated defence by the control of siRNA generation. The EMBO Journal **22,** 633–640.

Takeda A, Iwasaki S, Watanabe T, Utsumi M, Watanabe Y. 2008. The mechanism selecting the guide strand from small RNA duplexes is different among argonaute proteins. Plant and Cell Physiology **49,** 493–500.

Tian J, Pei H, Zhang S, Chen J, Chen W, Yang R, Meng Y, You J, Gao J, Ma N. 2014. TRV-GFP: a modified *Tobacco rattle virus* vector for efficient and visualizable analysis of gene function. Journal of Experimental Botany **65,** 311–322.

Turnage MA, Muangsan N, Peele CG, Robertson D. 2002. Geminivirus-based vectors for gene silencing in *Arabidopsis*. The Plant Journal **30,** 107–114.

Tuttle J, Idris A, Brown J, Haigler CD. 2008. Geminivirus-mediated gene silencing from *Cotton leaf crumple virus* is enhanced by low temperature in cotton. Plant Physiology **148,** 41–50.

Wang C, Cai X, Wang X, Zheng Z. 2006. Optimisation of *Tobacco rattle virus*-induced gene silencing in *Arabidopsis*. Functional Plant Biology **33,** 347–355.

Wang H, Huang Z, Chen Q, Zhang Z, Zhang H, Wu Y, Huang D, Huang R. 2004*a*. Ectopic overexpression of tomato *JERF3* in tobacco activates downstream gene expression and enhances salt tolerance. Plant Molecular Biology **55,** 183–192.

Wang H, Stier G, Lin J, Liu G, Zhang Z, Chang Y, Reid MS, Jiang CZ. 2013. Transcriptome changes associated with delayed flower senescence

on transgenic petunia by inducing expression of *etr1-1*, a mutant ethylene receptor. PLoS One **8,** e65800.

Wang JF, Zhou H, Chen YQ, Luo QJ, Qu LH. 2004*b*. Identification of 20 microRNAs from *Oryza sativa*. Nucleic Acids Research **32,** 1688–1695.

Wang XB, Jovel J, Udomporn P, Wang Y, Wu Q, Li WX, Gasciolli V, Vaucheret H, Ding SW. 2011. The 21-nucleotide, but not 22-nucleotide, viral secondary small interfering RNAs direct potent antiviral defense by two cooperative argonautes in *Arabidopsis thaliana*. The Plant Cell **23,** 1625–1638.

Wang XB, Wu Q, Ito T, Cillo F, Li WX, Chen X, Yu JL, Ding SW. 2010. RNAi-mediated viral immunity requires amplification of virus-derived siRNAs in *Arabidopsis thaliana*. Proceedings of the National Academy of Sciences, USA **107,** 484–489.

Yi SY, Kim JH, Joung YH, Lee S, Kim WT, Yu SH, Choi D. 2004. The pepper transcription factor CaPF1 confers pathogen and freezing tolerance in *Arabidopsis*. Plant Physiology **136,** 2862–2874.

Yin J, Chang X, Kasuga T, Bui M, Reid MS, Jiang CZ. 2015. A basic helix-loop-helix transcription factor, *PhFBH4*, regulates flower senescence by modulating ethylene biosynthesis pathway in petunia. Horticulture Research **2,** 15059.

Zhang H, Huang Z, Xie B, Chen Q, Tian X, Zhang X, Zhang H, Lu X, Huang D, Huang R. 2004. The ethylene-, jasmonate-, abscisic acid-and NaCl-responsive tomato transcription factor JERF1 modulates expression of GCC box-containing genes and salt tolerance in tobacco. Planta **220,** 262–270.

Zhang X, Yuan YR, Pei Y, Lin SS, Tuschl T, Patel DJ, Chua NH. 2006. *Cucumber mosaic virus*-encoded 2b suppressor inhibits *Arabidopsis* Argonaute1 cleavage activity to counter plant defense. Genes & Development **20,** 3255–3268.

Zhang X, Zhang X, Singh J, Li D, Qu F. 2012. Temperature-dependent survival of *Turnip crinkle virus*-infected *Arabidopsis* plants relies on an RNA silencing-based defense that requires DCL2, AGO2, and HEN1. Journal of Virology **86,** 6847–6854.

Zhao Y, Wei T, Yin KQ, Chen Z, Gu H, Qu LJ, Qin G. 2012. Arabidopsis RAP2.2 plays an important role in plant resistance to *Botrytis cinerea* and ethylene responses. New Phytologist **195,** 450–460.